Electron Trapping in Polar-Solvated Zeolites

Eric H. Ellison*

Department of Chemistry and Biochemistry, 322 Coulter Hall, University of Mississippi, University, Mississippi 38677

Received: July 1, 2005; In Final Form: September 6, 2005

Of current interest in our laboratory is the nature of photoinduced processes in the cavities of zeolites completely submerged in polar solvents, or polar-solvated zeolites (PSZ). The present study addresses the nature of electron trapping in PSZ with emphasis on the zeolites NaX and NaY. Free electrons were generated by two-photon, pulsed-laser excitation of either pyrene or naphthalene included in zeolite cavities. Trapped electrons were monitored by diffuse transmittance, transient absorption spectroscopy at visible wavelengths. In anhydrous alcohols, electron trapping by Na_4^{4+} ion clusters was observed in both NaX and NaY. The resulting trapped electrons decayed over the course of tens of milliseconds. No evidence for alcohol-solvated electrons was found. More varied results were observed in solvents containing water. In NaX submerged in CH_3OH containing 5% or higher water, species having microsecond lifetimes characteristic of solvated electrons were observed. By contrast, a 2 h exposure of NaY to 95/5 CH_3OH/H_2O had no effect on electron trapping relative to anhydrous CH_3OH. The difference between NaX and NaY was explained by how fast water migrates into the sodalite cage. Prolonged exposure to water at room temperature or exposure to water at elevated temperatures was necessary to place water in the sodalite cages of NaY and deactivate Na_4^{4+} as an electron trap. Additional studies in NaY revealed that solvent clusters eventually become lower energy traps than Na_4^{4+} as the water content in methanol increases. In acetonitrile−water mixtures, electron trapping by Na_4^{4+} was eliminated and no equivalent species characteristic of solvated electrons in methanol−water mixtures was observed. This result was explained by the formation of low energy solvated electrons which cannot be observed in the visible region of the spectrum. Measurements of the rate of O_2 quenching in anhydrous solvents revealed rate constants for the quenching of ion cluster trapped electrons that were 2−4 times higher than that for pyrene triplets. In NaX, the rate constant in methanol was 10^4 times smaller than that in cyclohexane, showing greater inhibition of O_2 reactivity in the medium of PSZ. The results of this study point out the conditions under which Na_4^{4+} is active as an electron trap in PSZ and that water must be present in the sodalite cage to produce solvated electrons in the supercage.

Introduction

The study of electron trapping in zeolites has spanned several decades and is important in the application of zeolites as storage media for radioactive pollutants and as reaction media for chemistry involving electron transfer. Initial studies by Kasai in 1965 showed that γ-ray or X-ray irradiation of dehydrated NaY in a vacuum produced a pink color center and a 13-line electron paramagnetic resonance (EPR) spectrum, both of which were attributed to trapped electrons in a site composed of four Na^+ ions in a "large" cavity.[1] In related studies, Rabo[2] and later Kasai and Bishop[3] showed that effusion of sodium vapor into the cavities of NaY produced essentially the same effect. In these systems, electron trapping occurs through the reaction $Na_4^{4+} + e^- \rightarrow Na_4^{3+}$, where Na_4^{4+} is the four-sodium ion cluster and Na_4^{3+} is the four-sodium, ion cluster trapped electron (heretofore referred to as e_{4s}^-). A recent account[4] has argued that Na_4^{4+} is located in the sodalite cage (or β-cage), a concept supported by the work of Barrer and Cole[5] who showed a similar trapping species in sodalite. The only cages found in sodalite are β-cages. Theoretical studies have modeled Na_4^{4+} on the basis of the sodalite structure and satisfactorily reproduced the electronic absorption spectrum of e_{4s}^-.[6,7] From these studies, changes in peak maxima on the basis of lattice effects were predicted and used to interpret lattice effects in other systems besides sodalite where Na_4^{4+} has been observed.

In more recent times, Thomas and co-workers have shown that e_{4s}^- can be generated photolytically, by two-photon excitation of aromatic species such as naphthalene located in the internal cavities of the zeolites NaX or NaY.[8−10] Far-UV photolysis,[11−13] γ-radiolysis,[14,15] and pulsed radiolysis[16] combined with EPR and UV−visible absorption spectroscopy were also used to identify various types of ion clusters and to characterize the stability and reactivity of ion cluster trapped electrons under various conditions. These studies were recently reviewed.[17,18] One issue pursued was the formation of hydrated electrons in the cavities of NaX and NaY. Hydrated electrons were found to be trapped by water clusters of varying size depending on the water content of the zeolite.

From the perspective of photochemistry in zeolites, the topic of electron trapping by ion and solvent clusters in zeolite cavities is important.[19] Ion clusters have been implicated in mechanisms of photoinduced electron transfer in zeolites, and may have a special role in electron transfer chemistry. One postulate is that ion clusters are involved in a type of superexchange mechanism, in which long-range electron transfer is enhanced between molecules located in adjacent supercages. Of importance are the conditions under which ion clusters are active and able to participate in photochemistry in zeolites.

* E-mail: eellison@olemiss.edu.

10.1021/jp053617h CCC: $30.25
Published on Web 10/12/2005

Of recent interest in our laboratory is the nature of photoinduced processes involving arenes in polar-solvated zeolites (PSZ), or zeolites completely submerged in either polar organic solvents or water. We have found that certain arenes cannot be easily extracted with desorbing polar solvents from the internal cavities of the zeolites NaX and NaY, despite the fact that they can easily be placed in the cavities by adsorption from nonpolar solvents. Larger arenes such as pyrene are particularly prone to the effect and remain in the zeolite for months at room temperature. Even smaller arenes such as naphthalene are, in some cases, only slowly extracted. The trapping effect allows for studies of photoinduced electron transfer involving aromatic species in the polar-solvated cavities of the zeolites X and Y. Of importance to these studies is the behavior of excess electrons and the conditions under which ion clusters are active in PSZ.

In the following, the behavior of excess electrons is examined in the zeolites NaX and NaY completely bathed in polar organic solvents containing variable amounts of water. Free electrons were generated by pulsed, two-photon excitation of either pyrene (PY) or naphthalene (NP) included in zeolite cavities. The propensity for Na_4^{4+} to trap electrons was evaluated from time-resolved measurements of electronic absorption spectra and decay profiles in the region 400−800 nm. One advantage of this approach over radiolysis is that the photolytic approach confines the excitation to the intraparticle domain of the zeolite. The bulk solvent surrounding the zeolite particles does not absorb the excitation light as in radiolysis, and therefore does not contribute to the measured signals.

The results of this study show that upon submerging NaX or NaY in anhydrous alcohols or acetonitrile, Na_4^{4+} remains active as an electron trap. The resulting trapped electrons exhibit behavior similar to that in solvent-free zeolites. More interesting results were observed in solvents containing water. Only water is small enough and polar enough to migrate through the sodalite apertures and into the sodalite cage where it can deactivate Na_4^{4+} as an electron trap. For the most part, this study seeks to explain the effects of water in solvents on the behavior of excess electrons in PSZ.

Experimental Section

Materials. Powdered forms of the zeolites NaX and NaY were obtained from Aldrich or UOP and have the chemical compositions $Na_{80}Al_{80}Si_{112}O_{384}$ (Si/Al = 1.4) and $Na_{55}Al_{55}Si_{137}O_{384}$ (Si/Al = 2.5), respectively. Both zeolites were stirred in excess 1 M $NaNO_3$(aq) and thoroughly rinsed with ultrapure Millipore water. Pyrene was purified by column chromatography using hexane as the mobile phase and activated silica gel as the stationary phase. The product of the separation was a pure white solid. Naphthalene was recrystallized from ethanol. HPLC-grade cyclohexane and anhydrous forms of methanol, ethanol, *n*-butanol, and acetonitrile initially containing <0.005% water were purchased and stored over activated, type 3A molecular sieves prior to use. Water was obtained from a Barnstead Nanopure delivery system.

Methods. Zeolite powders were pressed into thin (100 μm thick) pellets and dried in air at 550 °C for at least 15 min. The zeolite dry weight of samples ranged from 7 to 15 mg. After cooling the pellets under a flowing stream of dry N_2, they were transferred to solutions of either pyrene or naphthalene in cyclohexane and agitated for at least 2 h on an orbital shaker. For loadings <0.05 sc^{-1}, the loading procedure resulted in >95% adsorption. Loaded samples were transferred to 10 × 1 mm^2 evacuable suprasil cells and evacuated to milliTorr pressures at 125 °C for 15 min in order to remove the cyclohexane and small amounts of H_2O.

For studies of anhydrous solvent effects, the solvent was directly added to the thin cell containing the heat-treated (activated) zeolite sample in a glovebox. A subsequent study showed that similar results could be obtained simply by transferring the solvent in air, keeping exposure in air to a minimum (<5 s). For studies of solvents containing water, samples were agitated in 2.5 mL of solvent for at least 2 h.

Fourier transform infrared (FTIR) analysis of self-supported disks was carried out by using a Bruker IFS-66 spectrometer. A specially designed IR cell was constructed locally by utilizing 19 mm CaF_2 disks as windows of an evacuable 10 cm × 1 cm glass thin cell (0.1 cm thickness). Holes were drilled in each glass window near the bottom of the cell. The CaF_2 disks were placed over the holes and fastened vacuum-tight with epoxy. The sample disk was held horizontally in the cell while being heated and located such that the CaF_2 windows and epoxy material were not heated. Heating of the sample region was achieved by placing samples over the exhaust vent of a drying oven. Following thermal treatment of the sample disk, the cell was vertically positioned, which resulted in the disk falling to the bottom of the cell where the CaF_2 windows were located.

Electrons were generated in zeolites by excitation of either pyrene or naphthalene with a Continuum Surelite Nd:YAG pulsed laser (τ_{pulse} = 5 ns) operating at the fourth harmonic (266 nm). Spectra were measured by two different approaches. One approach utilized the laser pulse to trigger a gated, fiber-optic-coupled CCD array spectrometer and a pulsed analyzing light source (i.e., a xenon flashlamp, τ_{pulse} = 2 μs). This approach yielded the spectrum at 12 μs or longer following the laser pulse. The second approach triggered the CCD array spectrometer before the laser pulse and used as an analyzing light source a 50 ns plasma burst generated by focusing the fundamental of the Nd:YAG laser onto an aluminum plate. This approach yielded the spectrum at 100 ns following the laser pulse but in some cases was limited by fluorescence. In both approaches, the analyzing light was sufficiently intense to allow for measurements of optical density in the diffuse transmittance mode, where light transmitted through the sample disk was used as the analyzing light. All spectra were collected with a single laser pulse.

Decay profiles of optical density were also measured in the diffuse transmittance mode. The analyzing light source was either the steady-state or millisecond-pulsed output of a 450 W xenon arc lamp (Edinburgh Analytical Instruments Xe900 and Xp900). An Oriel model 77200 monochromater was used to select the analyzing wavelength, and a Hamamatsu R955 photomultiplier tube was used as the detector.

Results

Infrared Analysis of Zeolitic Water. An important issue in this study is whether the thermal treatment used to remove water from zeolite samples is effective. Therefore, an infrared spectroscopic study of zeolitic water was carried out. An evacuable IR cell was constructed as described in the Experimental Section and was designed to simulate conditions under which samples in quartz thin cells were dehydrated.

The infrared absorption spectrum of NaY subjected to evacuation for 15 min at 125 °C is shown in Figure 1 (upper panel). For comparison, a sample containing 5% added water is also shown. The most notable bands have been assigned by Breck[20] and Ward.[21] Free water is indicated by the bands at 1645 cm^{-1} (bending mode), 3460 cm^{-1} (stretching mode), and 3250 cm^{-1} (stretching mode). The band at 3695 cm^{-1} originates from isolated hydroxyl groups. While NaY is nearly completely

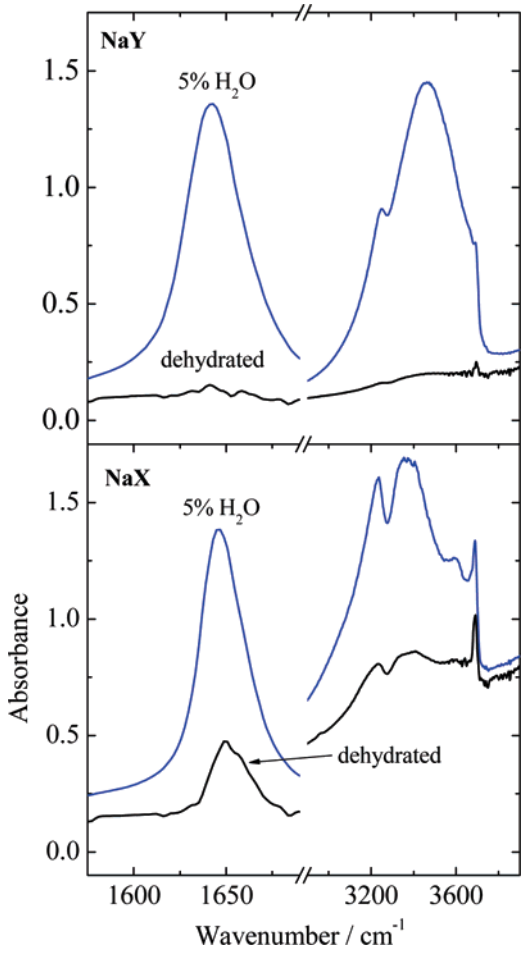

Figure 1. Infrared absorption spectrum of NaX and NaY containing variable amounts of water.

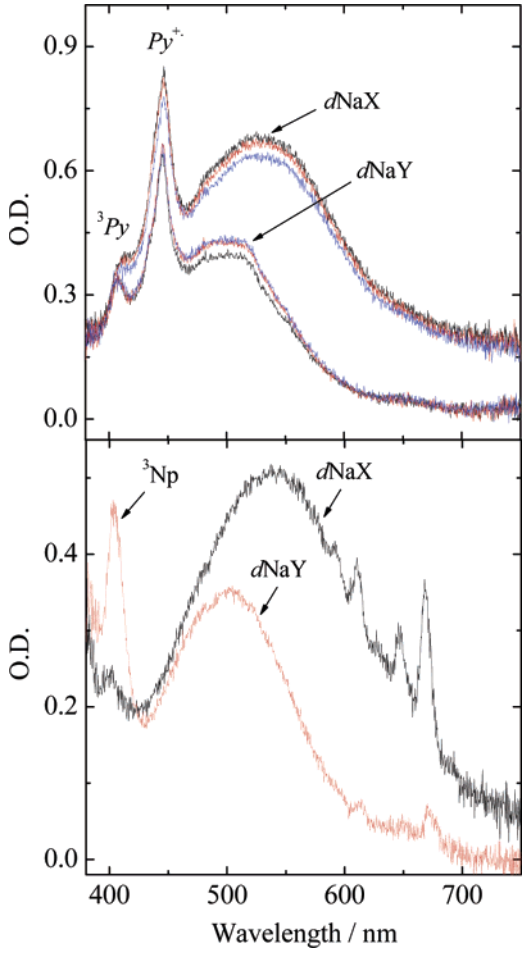

Figure 2. Absorption spectrum at 12 μs following 2 $h\nu$ excitation of pyrene (upper graph) or naphthalene (lower graph) in dNaX and dNaY. λ_{ex} = 266 nm. Loadings = 0.002 sc^{-1} (PY) and 0.04 sc^{-1} (NP).

dehydrated following the thermal treatment, NaX shows 1% or less residual water. Tighter association of water with NaX is expected, since NaX has a greater number of exchangeable sodium ions than NaY.

More than 40 years ago, an IR analysis was carried out on Linde molecular sieve X.[22] The reported IR spectrum was very similar to the one observed here. The earlier study also showed that heating NaX at 100 °C for 20 h under vacuum produced 0.10 H_2O/cavity (or 0.11% H_2O). Therefore, for the purposes of the current study, the thermal treatment used is effective at removing water from samples. Attention is now focused on studies of electron trapping.

Electron Trapping in Zeolites. As originally shown by Thomas and co-workers, two-photon excitation of arenes included in dehydrated, solvent-free NaX and NaY (or dNaX and dNaY) generates stable arene cation radicals and ion cluster trapped electrons.[8−10] Figure 2 illustrates the effect following 2 $h\nu$ excitation of either pyrene (PY) or naphthalene (NP). Each spectrum was collected at 12 μs following a single laser pulse. As shown in the upper graph where PY was used, pulse-to-pulse errors were about 10% in amplitude. The broadened bands peaking at 504 nm in NaY and 540 nm in NaX can be assigned to trapped electrons and are overlapped by pyrene triplet (^{3}Py) bands at 410 and 520 nm and by the pyrene radical cation ($Py^{+\bullet}$) and radical anion ($Py^{-\bullet}$) at 445 and 490 nm, respectively. The bands at 490 and 520 nm are weak and hardly observable in the spectra. The lower graph illustrates the spectra measured by using NP as an electron source. The bands in the region 580−700 nm originate from the naphthalene radical cation. Triplet NP is observable at 405 nm. In NaX, the triplet band is less conspicuous most likely because of triplet−triplet annihilation. Such effects were observed previously for anthracene.[23] Radiolysis studies have shown the spectrum of e_{4s}^- to peak at 535 and 505 nm in NaX and NaY, respectively, consistent with the present results. In evacuated samples of both NaX and NaY, the decay time of e_{4s}^- was in the range of tens of milliseconds, depending on residual O_2 pressure. As previously shown, recombination of $Py^{+\bullet}$ and e_{4s}^- does not occur on microsecond or longer time scales in these systems.[24] Essentially, $Py^{+\bullet}$ and e_{4s}^- are immobile over the lifetime of e_{4s}^-.

In the following, electron trapping and solvation in zeolites completely submerged in alcohols and acetonitrile of variable water content is described.

NaX−Methanol. In NaX, electron trapping by Na_4^{4+} was essentially unaffected by submersion of anhydrous samples in CH_3OH. Figure 3 illustrates the absorption spectrum at 12 μs following excitation of PY in NaX. Decay profiles at 560 nm are also shown. The graphs refer to two different samples bathed in CH_3OH: one in which anhydrous CH_3OH was added to anhydrous samples (referred to as aCH_3OH) and another that was thoroughly rinsed with anhydrous CH_3OH following exposure to H_2O (referred to as rCH_3OH). Prolonged (several hours) exposure to CH_3OH was not a factor in the rCH_3OH data. The rCH_3OH data are explained in detail below. In aCH_3-OH, a broadened band characteristic of e_{4s}^- is clearly visible but is less broadened compared to dNaX. Measurements of

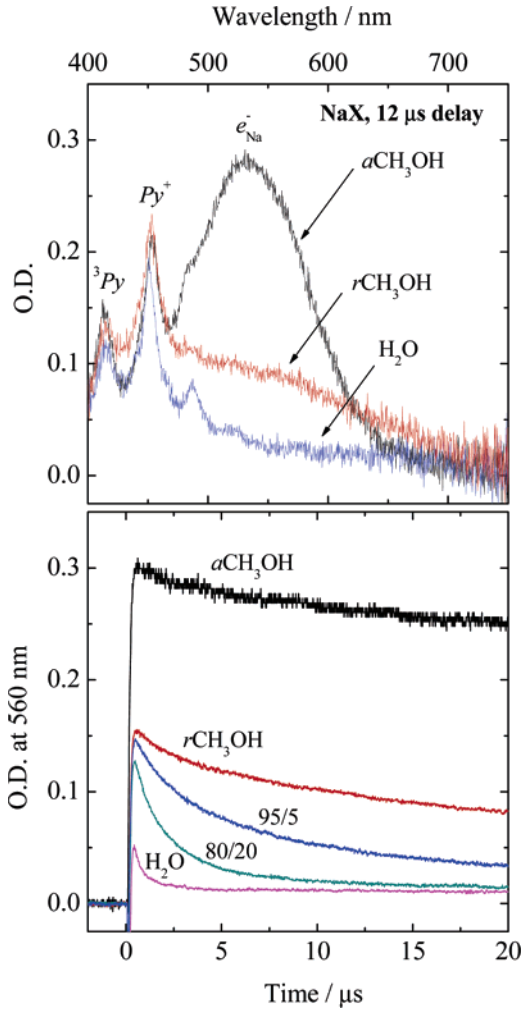

Figure 3. Absorption spectra and microsecond decay profiles following 2 $h\nu$ excitation of pyrene in methanol-solvated NaX. See text for further details.

decay profiles at 560 nm revealed a decay time of 18 ms after bubbling with N_2. The decay profiles in CH_3OH-H_2O mixtures were dominated by "microsecond components" having decay times <20 μs. For this reason, the 12 μs spectra of these samples appeared much the same as in water, with the exception of 95/5 CH_3OH/H_2O. Decay profiles of $Py^{+\bullet}$ were also measured and showed no microsecond decay components that could possibly result from recombination of electrons with $Py^{+\bullet}$. Bubbling the samples with N_2 had no effect on the decay profiles shown in Figure 3. However, on millisecond or longer time scales, the decay profile in aCH_3OH was sensitive to O_2 concentration which allowed for measurements of the rate of quenching by O_2 (see below).

Of further importance in Figure 3 is that the yield of $Py^{+\bullet}$ is an indicator of how many free electrons were produced. The only source of $Py^{+\bullet}$ is from two-photon ionization. Thus, the decrease in optical density (OD) at 560 nm that occurred as a result of adding water to CH_3OH is not the result of lowered free electron yields, since the yield of $Py^{+\bullet}$ was essentially constant throughout. Another important aspect of the results in Figure 3 was that in H_2O the microsecond decay component decayed into a nonzero baseline. The origin of this residual OD is unclear but could be due to laser heating that results in optical effects or slight changes in refractive index. The nonzero baseline was a common trait in other systems as well.

The spectrum of the microsecond components in Figure 3 is of interest and may comment on their origin, that is, whether they originate from ion cluster electrons or solvated electrons. Using the present setup, collection of spectra on time scales <12 μs required that the CCD spectrometer be triggered before the laser flash, as opposed to after as in Figure 3. By using this approach and PY as an electron source, spectral distortion from fluorescence was a problem. For this reason, NP was utilized as an electron source, since NP fluorescence occurs at shorter wavelengths than PY. While this approach worked for $NaX-CH_3OH$, it was not generally applicable to all systems. For example, in NaY, NP was completely extracted within a few minutes in all polar solvents. In $NaX-CH_3OH$, extraction occurred more slowly, over the course of hours, probably due to the higher viscosity in NaX.

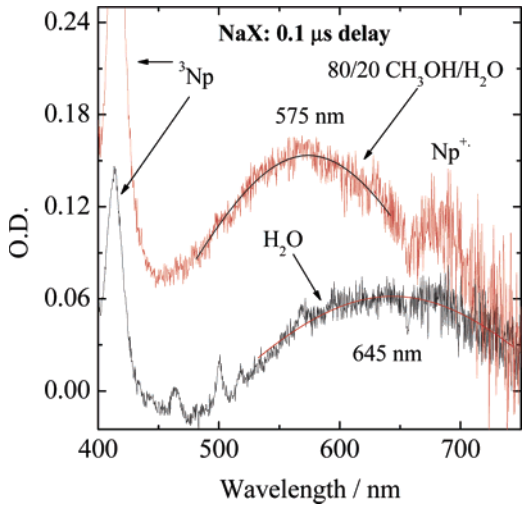

Figure 4. Absorption spectra at 0.1 μs following 2 $h\nu$ excitation of naphthalene in NaX submerged in either 80/20 CH_3OH/H_2O or H_2O.

Spectra of the microsecond components measured at 0.1 μs after the laser pulse are illustrated in Figure 4. Triplet NP is observable in the spectrum at 415 nm as well as overlapping peaks from the NP radical cation. In 80/20 CH_3OH/H_2O, the absorption maximum occurs at 575 nm, which is red-shifted by 40 nm to the spectrum in $NaX-CH_3OH$. In H_2O, the spectrum is similar to that observed by Thomas and co-workers in fully hydrated NaX and is blue-shifted by about 55 nm to that observed for hydrated electrons in bulk water. The spectrum in 40/60 CH_3OH/H_2O was also measured and showed a similar amplitude response to that in water. For display purposes, these data were not included in the graph but showed an absorption maximum at 615 nm. Thus, the absorption maximum of the microsecond component increased and the decay time became shorter with increasing H_2O content. If these are solvated electrons, then in mixed solvents both CH_3OH and H_2O contribute to solvation and CH_3OH causes elongated decay times.

In other anhydrous alcohols including ethanol and *n*-butanol, a similar response to that in aCH_3OH in Figure 3 was observed. However, the response to added water was different. For example, the results in 95/5 $BuOH/H_2O$ in terms of decay times and 0.1 μs spectra were characteristic of the results in $NaX-H_2O$. This indicates that BuOH does not compete effectively with H_2O for the zeolite interior. This is expected because the zeolite itself is quite polar and would favor absorption of the more polar solvent.

Figure 5 compares the pyrene fluorescence spectrum in aCH_3OH and rCH_3OH. Pyrene fluorescence is a well-established probe of microenvironment polarity or solvent dipole moment in the III/I peak intensity ratio.[25] The III/I ratio of 0.68 in rCH_3-

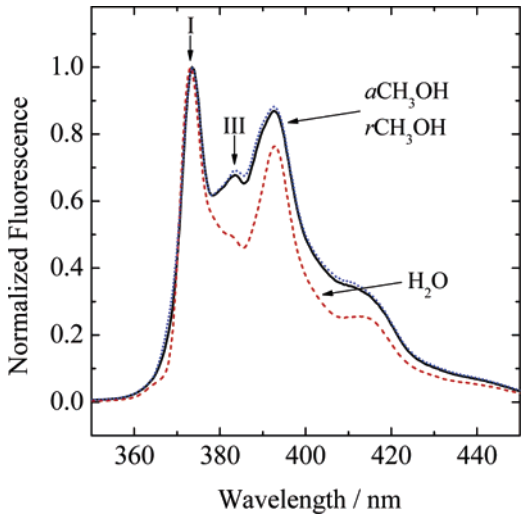

Figure 5. Fluorescence spectrum of pyrene in NaX submerged in methanol or water. See text for further details.

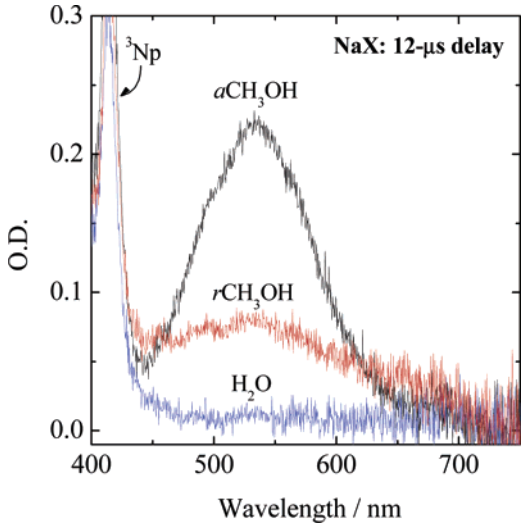

Figure 6. Spectra following 2 *hν* excitation of naphthalene in solvated NaX.

OH was essentially equivalent to that in aCH_3OH. Further, the III/I ratio was significantly different in aCH_3OH and H_2O, which indicates sensitivity to solvent properties. Given these results, the effects of water on pyrene photophysics can be described as reversible. By contrast, the results in Figure 3 do not indicate reversibility. A reasonable explanation is that exposure to H_2O fills the sodalite cages with H_2O to eliminate electron trapping by Na_4^{4+}. A subsequent CH_3OH rinse removes H_2O from the supercage but not the sodalite cage.

Returning to Figure 3, the broadened band in rCH_3OH is of interest. The spectrum of this band was further assessed by using NP, to eliminate spectral overlap from $Py^{+\bullet}$. A spectral comparison at 12 μs is illustrated in Figure 6. In these spectra, the NP triplet is observable at 415 nm because annihilating reactions are slowed due to the lowered mobility of NP. While the peak maximum of the broadened band in rCH_3OH is similar to that in aCH_3OH, more broadening occurred in rCH_3OH and the lifetime was much shorter ($\tau = 245$ μs). The band in rCH_3OH could originate from either CH_3OH-solvated electrons or ion cluster electrons. Dorfman reported the spectrum of solvated electrons in bulk CH_3OH to peak at 630 nm.[26] Although this peak maximum is red-shifted from the band observed here, 0.3 eV blue shifts have been observed here and elsewhere for hydrated electrons in NaX compared to bulk water. On the other

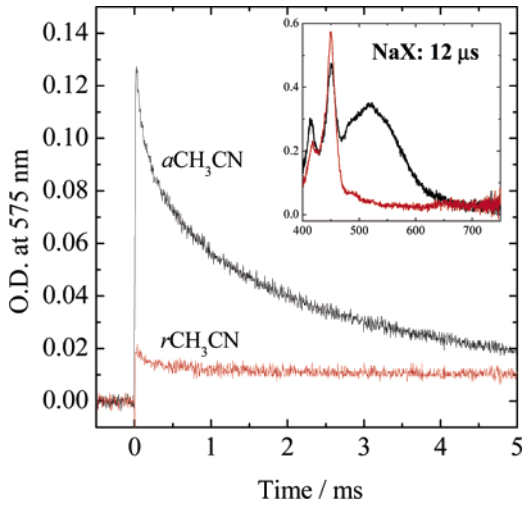

Figure 7. Millisecond decay profiles and absorption spectra following 2 *hν* excitation of pyrene in NaX submerged in acetonitrile.

hand, Dorfman reported bulk lifetimes in the range 1−5 μs at room temperature. Thus, the elongated lifetime in rCH_3OH is difficult to explain. Trapping by ion clusters cannot be ruled out. The data in acetonitrile are of use in interpreting the results in CH_3OH and are described in the following.

NaX−Acetonitrile. Figure 7 illustrates the spectra and decay profiles observed in NaX bathed in acetonitrile. The designations aCH_3CN and rCH_3CN are defined similarly to those in Figure 3 for CH_3OH. In aCH_3CN, the OD of e_{4s}^- was approximately the same as that in aCH_3OH, although the $Py^{+\bullet}$ yield was much higher. Thus, for a given yield of $Py^{+\bullet}$, the yield of e_{4s}^- was lower in CH_3CN. A similar effect was observed in NaY (see below). In rCH_3CN, no broadened band similar to that in rCH_3OH was observed; the ODs in the spectral region of e_{4s}^- were very low, and a decay analysis revealed no microsecond components out to 750 nm that would have gone undetected in the 12 μs spectra. A similar result was observed in 95/5 CH_3CN/H_2O. One possibility is that solvated electrons are present in these systems but cannot be detected with the present apparatus. Previous radiolysis studies have shown that solvated electrons absorb at 1500 nm in bulk CH_3CN at room temperature.[27,28] However, in 80/20 CH_3CN/H_2O, decay profiles revealed a microsecond component with a lifetime of 2.8 μs and a 0.1 μs spectrum characteristic of that observed in H_2O in Figure 4. This may indicate that water is preferentially absorbed by NaX over CH_3CN and that in 80/20 CH_3CN/H_2O enough water is present to swamp out the effects of CH_3CN.

For comparison, measurements made in NaX were similarly made in NaY. The results indicate both similarities and differences between the two materials.

NaY−Methanol. Figure 8 illustrates the spectra and decay profiles observed following excitation of pyrene in NaY. Compared to NaX, higher water contents were required to eliminate the millisecond-lived component in NaY. For example, results in 95/5 CH_3OH/H_2O were identical to those in aCH_3OH and both millisecond and microsecond components were observed in 80/20 CH_3OH/H_2O. Interestingly, the results in rCH_3OH were essentially the same as those in aCH_3OH, meaning that the effects of H_2O were reversible in NaY. This implies that H_2O does not enter the sodalite cages of NaY at an appreciable rate, at least over the course of the 2 h exposure used here.

The possibility that water does not enter the sodalite cage in NaY was further explored through studies of temperature effects

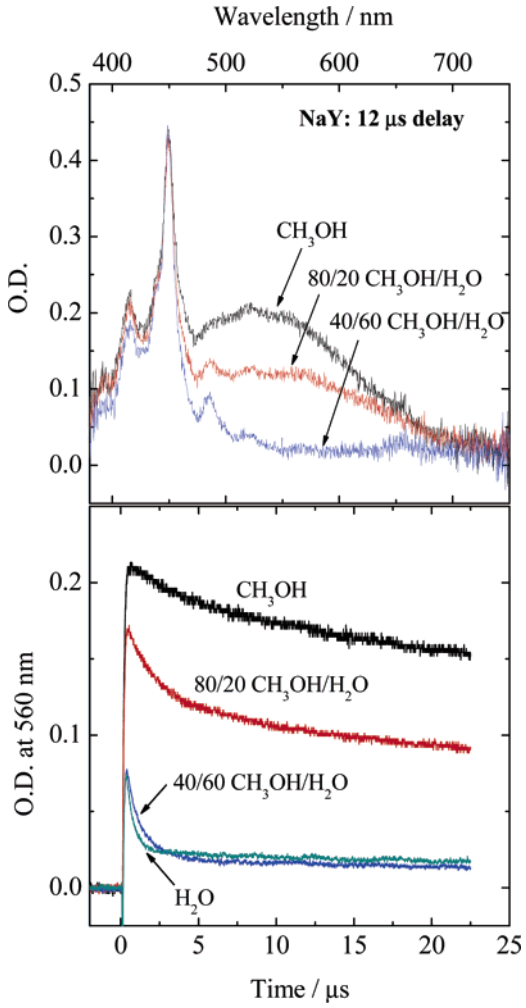

Figure 8. Absorption spectra and microsecond decay profiles following 2 $h\nu$ excitation of pyrene in methanol-solvated NaY.

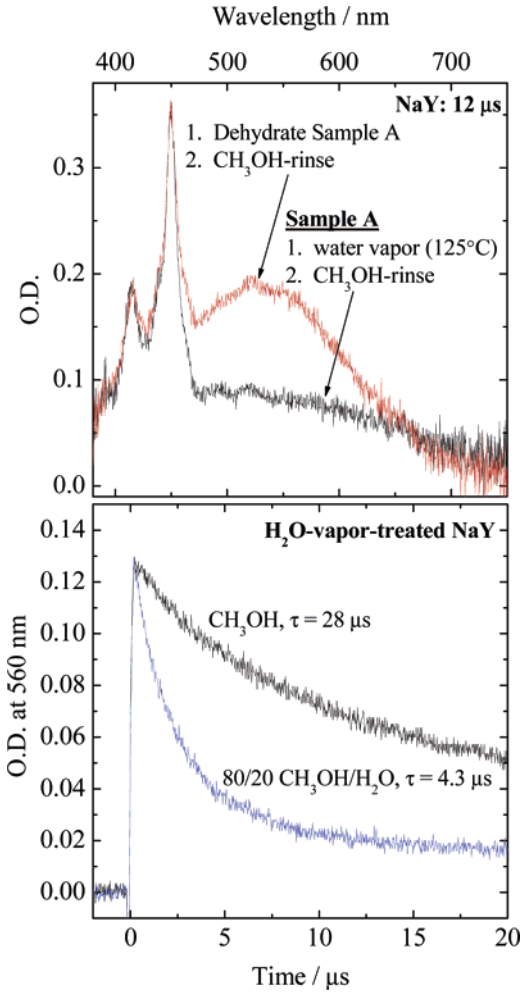

Figure 9. Effects of the water-vapor treatment on the spectrum and decay profile of trapped electrons in methanol-solvated NaY.

during exposure to H_2O. Figure 9 illustrates the results. The treatment consisted of initially submerging a sample disk containing pyrene in water, followed by transfer of the wet disk to an evacuable cuvette. Subsequently, the sample was evacuated at room temperature for 1 min to remove air and then heated at 125 °C with the vacuum tap closed for 30 min. Water was clearly present in the cuvette during the heating step, as evidenced by condensate on cooler parts of the cell. Following the water-vapor treatment, the sample was thoroughly rinsed in anhydrous CH_3OH to yield sample A, the results for which were dissimilar to those in aCH_3OH. In many ways, the results were similar to the results in NaX in rCH_3OH—the 560 nm decay time was much shorter, and the yields were lower compared to aCH_3OH. If sample A was subsequently placed in 80/20 CH_3OH/H_2O, the decay time became even shorter. If sample A was evacuated to dryness at 125 °C for 15 min and rinsed once again in anhydrous CH_3OH, results similar to those in aCH_3OH were observed. The upper graph in Figure 9 shows the results. The same vapor treatment used on NaY was also applied on NaX but produced no changes relative to rCH_3OH in Figure 3. These results imply that migration of H_2O into the sodalite cage has a higher activation energy in NaY compared to NaX.

Of notable interest was the effect of allowing samples to equilibrate in water at room temperature. If a NaY disk containing PY was exposed to water for 4 days, a purely arbitrary time period, results similar to the water-vapor treatment were observed. Therefore, at room temperature, water migrates into the sodalite cages of NaY but at a much slower rate compared to NaX. A subsequent study showed that submerging NaY in water at 90 °C expedites the process.

One other topic of interest in CH_3OH is the nature of pyrene fluorescence in NaY. Unlike the result in NaX where the effects of water were reversible in rCH_3OH, significant differences between aCH_3OH and vapor-treated NaY were observed. The results for NaY are illustrated in Figure 10. Vapor-treated samples that were rinsed with CH_3OH showed a significantly higher III/I ratio than either aCH_3OH or rCH_3OH. Even in water, the III/I ratio was higher relative to the untreated sample. Similar results to the vapor treatment were observed if the samples were allowed to stand in water for several days. These observations refute the idea that water in the sodalite cage has no impact on pyrene photophysics. The different fluorescence responses in NaX and NaY are addressed in the Discussion.

In NaY−CH_3CN, the 12 μs spectrum appeared essentially the same as that in NaY−CH_3OH, with the only difference being a 25% reduction in the yield of e_{4s}^-. As in CH_3OH, the effects of water were reversible upon rinsing aqueous NaY with anhydrous CH_3CN. The main difference between CH_3CN and CH_3OH was the response to added H_2O. In 95/5, 80/20, and 40/60 CH_3CN/H_2O, the results were essentially the same—the 12 μs spectrum was eliminated, and microsecond components were not observed anywhere in the region 550−750 nm. In essence, the results were similar to those observed in NaX in rCH_3CN and 95/5 CH_3CN/H_2O. However, the species observed in NaX in 80/20 CH_3CN/H_2O was not observed in NaY, even

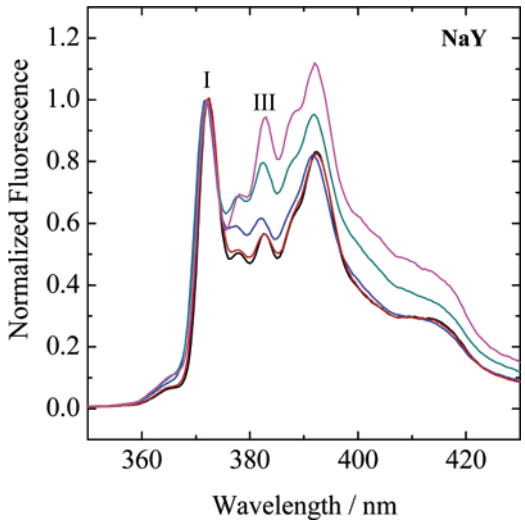

Figure 10. Effects of the water-vapor treatment on the spectrum of pyrene fluorescence in methanol-solvated NaY and aqueous-solvated NaY. At 383 nm from top to bottom: CH_3OH (vapor-treated); H_2O (vapor-treated); H_2O; rCH_3OH; aCH_3OH. $\lambda_{ex} = 337$ nm.

in 40/60 CH_3CN/H_2O. This may indicate that water more effectively accumulates over CH_3CN in the cavities of NaX compared to NaY.

In anhydrous CH_3OH and CH_3CN, the ion clusters are intact and able to trap electrons. Of interest is the rate of quenching of e_{4s}^- by O_2 in these systems. In the following, rate constants for the quenching of e_{4s}^- and pyrene triplets are compared.

O_2 Quenching. Figure 11 illustrates the decay profiles of e_{4s}^- in NaX−CH_3CN at various O_2 concentrations and provides an example of the type of data used to evaluate rate constants for quenching by O_2. Pyrene was used as a source of electrons. The samples were bubbled with N_2-O_2 mixtures to achieve a given O_2 concentration. The decay profiles of e_{4s}^- were heterogeneous and fit to a Gaussian model which assumes a Gaussian distribution in the natural logarithm of decay rates. More details on this approach are available elsewhere.[29,30] Essentially, the Gaussian approach provides a convenient means of determining the average decay rate and also provides an indicator of the degree of decay rate dispersion in values of γ.

Table 1 lists the rate constants for quenching of e_{4s}^- by O_2. In all cases, comparisons were made to the rate of pyrene triplet quenching by O_2, except in NaY−cyclohexane where the triplet yield was very low. In all cases, rate constants were calculated from Stern−Volmer plots of the decay rate versus $[O_2]$, as shown. $[O_2]$ was calculated by using literature values for the solubility of O_2 in various solvents at room temperature.[31] Thus, the rate constants are expressed on the basis of $[O_2]$ in solution. Since the solubility in solvated zeolite interiors may not necessarily be identical to that in bulk solution, the rate constants may not accurately reflect differences in O_2 mobility between systems. A drop in rate constant could result from either lowered solubility or lowered mobility of O_2. Thus, differences in O_2 mobility can only be discussed with the assumption that the O_2 solubility in zeolite interiors is the same as (or close to) that in bulk solution. However, comparisons of triplet and e_{4s}^- quenching in a given system are not affected by these assumptions.

The values in Table 1 show that rate constants for quenching of ^3Py are 2−4 times smaller than those of e_{4s}^-. On the basis of statistical considerations, the triplet rates can be taken as one-ninth the diffusion-controlled rate.[32] Thus, the rate of quenching of e_{4s}^- is 2−4 times smaller than the diffusion-controlled rate. This difference is much smaller compared to that previously

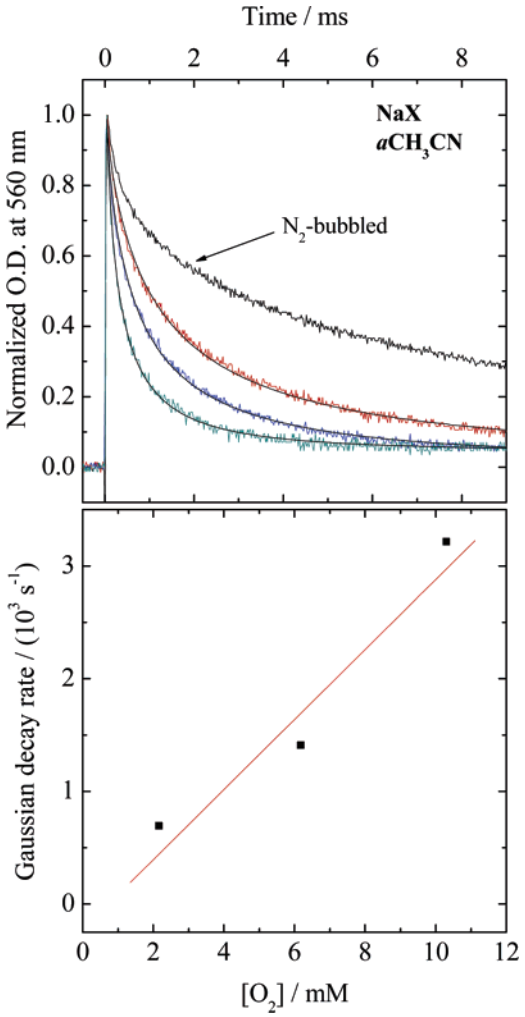

Figure 11. Example decay profiles and Stern−Volmer plot used in assessing rate constants for quenching by O_2.

TABLE 1: Rate Constants for Quenching by O_2 in Polar-Solvated NaX and NaY[a]

	NaX/NaY $k_q/(10^5\ s^{-1}\ M^{-1})$		
species	C_6H_{12}	CH_3CN	CH_3OH
e_{4s}^-	1400	3.5	0.14
	5000	41	26
^3Py	670	0.88	0.055
	n/a	11	9.8

[a] Rate constants were calculated on the basis of $[O_2]$ in solution. See text for further details.

measured at the gas−solid interface where the rate of quenching of e_{4s}^- was 200 times less than the diffusion-controlled rate, or 200 times less than the rate of quenching of pyrene fluorescence.[24] Since the quenching involves long-range electron transfer to yield superoxide, solvation by polar solvents may be a factor. However, similar effects were observed in cyclohexane. A reasonable explanation is that solvent cage effects are important in the reaction of e_{4s}^- with O_2. Cage effects would increase the residence time of O_2 in supercages adjacent to sodalite cages containing e_{4s}^-. Such effects would be observed in both polar and nonpolar solvents.

In cyclohexane, the rate constants were 2−4 orders of magnitude larger than those in CH_3OH and CH_3CN. That these differences could result entirely from differences in O_2 solubility seems unlikely, since O_2 solubility in bulk cyclohexane is only about 10−20% higher than that in bulk CH_3OH or CH_3CN.

Regardless, a more viscous bulk solvent would lower both the solubility and mobility of O_2. These results indicate severe restrictions on mobility in PSZ, even for a small, gaseous species such as O_2.

In polar solvents, the rate constants in NaY were larger than those in NaX. For example, in CH_3CN, the rates in NaY were 12 times larger than those in NaX. In CH_3OH, they were 180 times larger. While solvent structure in zeolite cavities is zeolite-specific and difficult to interpret, the smaller rate constants in NaX can be attributed to increased viscosity due either to hydrogen bonding or to ion−dipole interactions. The results in Table 1 are in qualitative agreement with recent measurements made in our laboratory of the rates of extraction of naphthalene from PSZ. In NaX−CH_3OH, extraction occurred over the course of 3 h compared to 30 min for NaX−CH_3CN. In NaY, extraction was complete within 5 min using either solvent.

Discussion

The present study shows that Na_4^{4+} is an active electron trap in NaX or NaY submerged in alcohols or acetonitrile. This result is in accord with a previous study where CH_3OH was added to dehydrated zeolites from the vapor phase.[33] To further test this result and describe its generality, two other polar solvents were examined, including dimethyl sulfoxide (DMSO) and *N*,*N*-dimethylformamide (DMF). On the basis of dielectric constants, both solvents are more polar than either CH_3OH or CH_3CN. Also, values of the standard molar Gibbs energies of transfer of sodium ions from water are negative for DMSO and DMF and positive for CH_3OH and CH_3CN, meaning that sodium ions are better solvated in DMSO and DMF than water.[34] Despite these properties, electron trapping by Na_4^{4+} was observed in both DMSO and DMF. Evidently, interactions of polar organic solvents with site II sodium ions do not greatly influence Na_4^{4+} as an electron trap.

When NaX and NaY were submerged in water, results consistent with previous studies[16,17] describing the formation of hydrated electrons in supercages were observed. Hashimoto and co-workers have debated whether these are actually hydrated electrons or small, unstable ion cluster trapped electrons such as Na_3^{2+} or Na_2^{+}.[33,35] The location of these ion clusters is unknown. Thomas argued for hydrated electrons on the basis of microsecond lifetimes which are consistent with that observed in bulk water and clearly different from that of ion cluster trapped electrons. They also showed that the "hydrated electrons" were dynamically quenched by methyl viologen (MV^{2+}) and that quenching was only possible above a threshold water content which allowed for cage-to-cage motion of water cluster electrons.

One interesting result observed here was that following a 2 h exposure of NaY to water at room temperature, a CH_3OH rinse reversed the effects of water and reactivated Na_4^{4+}. This was explained on the basis that water does not enter the sodalite cages of NaY when the time period of exposure to water is not very long. Nonetheless, in NaY submerged in water and devoid of water in the sodalite cage, the microsecond decays previously claimed to originate from either hydrated electrons or Na_3^{2+} and Na_2^{+} trapped electrons were observed. This implies either that Na_4^{4+} is destabilized as an electron trap by water located in the supercage or that Na_4^{4+} is not destabilized by water and that other trapping species such as Na_3^{3+}, Na_2^{2+}, or water clusters are lower energy traps than Na_4^{4+}. The latter is difficult to prove conclusively. At best, there is great difficulty in computing the energies of ion cluster electrons and solvated electrons in these systems. If the former is true, then H_2O located in the supercage must have a more destabilizing effect on Na_4^{4+} than organic solvents. Perhaps water, being smaller and of higher polarity than any of the organic solvents tested, can more effectively coordinate to site II cations from within the supercage. However, the slow rate of migration of water into the sodalite cages of NaY implies that solvation of site II cations from within the supercage is not very effective. In order for water to migrate into the sodalite cage, sodium ions must be displaced from the sodalite apertures. In NaY, this process is more activated than in NaX. In NaX, site II cations are apparently more loosely held, allowing water to more easily migrate into the sodalite cage. This can be explained by the well-known higher basicity of NaX compared to NaY.[36,37] Site II cations are less acidic in NaX.

If Na_4^{4+} retains its dry character in aqueous-solvated NaY, then the microsecond component originate from electron traps lower in energy than Na_4^{4+}. One possible explanation is that in water Na_3^{3+} or Na_2^{2+} becomes the main trapping species over Na_4^{4+} and is formed only in water. However, this is unlikely because these species are not the main trapping species in the absence of water, and Na_3^{3+} trapped electrons have been observed in both dNaX and dNaY. A more likely explanation is that the species in aqueous NaY is a solvated electron, as proposed by Thomas and co-workers.

The presence of water in the sodalite cages of NaX and NaY had a interesting effect on electron behavior. In NaX, a broadened band with $\tau = 245\ \mu$s and located near the region of e_{4s}^{-} was observed in rCH_3OH. A similar species was observed in NaY when water was placed in the sodalite cage by heating, although a much shorter lifetime of 28 μs was observed. An important question is whether this species is a solvated electron or ion cluster trapped electron. One notable result in NaX was that no species characteristic of that in rCH_3OH was observed in rCH_3CN. If the species in rCH_3OH is an ion cluster, then an explanation for why this ion cluster was not observed in rCH_3CN is required. A likely explanation is that with water in the sodalite cage and CH_3CN in the supercage, electrons are solvated by CH_3CN and not spectroscopically observable. Such solvated electrons would have to be lower energy electron traps than ion clusters. Whether this is actually the case is presently unclear.

One possible explanation is that the species in rCH_3OH is a solvated electron and that placing water in the sodalite cage simply eliminates electron trapping by ion clusters. While the relatively long lifetime in rCH_3OH is uncharacteristic of bulk solvated electrons, the rigid solvent structure in zeolite cavities could lead to stabilization of e_s^{-}, similar to the effects of low temperature in bulk solvents. In NaY, there are fewer cations to limit the mobility of CH_3OH. This could explain the shorter lifetime in NaY noted above and is supported by measurements of O_2 quenching where rate constants for quenching were about 20 times higher in NaY compared to NaX. In NaX, the incremental addition of water to CH_3OH decreased the lifetime of the microsecond component and shifted the absorption band to the red, eventually giving hydrated electrons. For example, in NaX, the species in 95/5 CH_3OH/H_2O had a shorter lifetime than that in rCH_3OH but appears to be derived from the species in rCH_3OH as the decay profiles indicate (see Figure 3). The decrease in lifetime can be explained by the increased mobility of water due to its small size.

Further discussion of differences between NaX and NaY is necessary. In NaX, the presence of even small amounts of water in CH_3OH eliminated electron trapping by Na_4^{4+}. The results in NaY were much different. Following a 2 h exposure of NaY

to 95/5 CH_3OH/H_2O, behavior similar to that in aCH_3OH was observed. This shows that small amounts of H_2O in CH_3OH can be tolerated in NaY, at least for short time periods, without deactivation of Na_4^{4+}. In 80/20 CH_3OH/H_2O, microsecond-lived components characteristic of solvated electrons and millisecond-lived components characteristic of e_{4s}^- were simultaneously observed. This can be explained by differing energies of the species involved. As more water is added to CH_3OH, solvated electrons become lower in energy than e_{4s}^-. In 80/20 CH_3OH/H_2O, these species are isoenergetic. Further explanation is needed to account for the results in CH_3CN. For example, in NaY, 5% water in CH_3CN essentially eliminated electron trapping by Na_4^{4+}. If this is the result of Na_4^{4+} deactivation by water in the supercage, then the argument must be made that CH_3OH is more competitive with water than CH_3CN for site II cations. This is unlikely because both solvents are of similar polarities. A more likely explanation is that small amounts of water in CH_3CN promote the formation of solvated electrons. Exactly how this occurs is unknown. More research is needed to describe the results in CH_3CN, in particular whether solvated electrons can be observed in the infrared region of the spectrum. The present study clearly shows the solvent conditions under which Na_4^{4+} is an active electron trap in these systems.

The difference in pyrene fluorescence in NaX and NaY also requires explanation. A large change in pyrene fluorescence occurred upon the placement of water in the sodalite cage of NaY by heating. This had relatively little effect in NaX. This difference might be explained by the impact of exchangeable cations on the solvent configuration controlling the pyrene microenvironment. Site II cations are the only cations which directly impact pyrene solvation in NaY. In NaX, site II cations as well as site III cations which are located near the supercage aperture could also impact solvation. The occupation of water in the sodalite cage may lessen the impact of site II cations on the solvent configuration in the supercage to yield more bulklike solvent behavior. In NaX, this effect is not observed because the impact of site II cations is swamped out by other ionic effects. We are presently examining solvation effects in more detail through fluorescence probing in a variety of solvents and zeolites.

Summary and Conclusions

The results of this study show that Na_4^{4+} in the zeolites NaX and NaY retains its activity as an electron trap when the zeolite is submerged in polar organic solvents including alcohols, acetonitrile, DMSO, and DMF. The resulting ion cluster trapped electrons were shown to be relatively stable, having lifetimes in N_2-bubbled solvents in the range of tens of milliseconds. When H_2O was deliberately added to the solvent, the behavior of trapped electrons varied depending on the Si/Al ratio of the zeolite, solvent, and water content. While water can enter the sodalite cage and deactivate Na_4^{4+} as an electron trap, organic solvents cannot. In methanol−water mixtures, species characteristic of solvated electrons were observed. More research is needed to describe results in acetonitrile where solvated electrons may be detectable in the infrared region of the spectrum.

One particularly interesting result was observed in NaY, where the effects of H_2O were reversible upon rinsing aqueous NaY with either methanol or acetonitrile. This result implies that exposure of NaY to water at room temperature does not immediately result in the occupation of water in the sodalite cage. Evidently, there is a considerable activation barrier to water migration into the sodalite cage. This result is important because it differs from conventional wisdom which states that water enters the sodalite cage rapidly.

The results of this study show important effects due to the presence of water in the sodalite cage. When water was placed in the sodalite cage resulting in the elimination of Na_4^{4+} as an electron trap, solvated electrons became observeable, even in anhydrous solvents. In organic solvent−water mixtures, the solvated electrons exhibited a character intermediate between that of pure water and anhydrous solvent. In NaY, solvated electrons formed even when water was not present in the sodalite cage, as solvent clusters became lower energy traps than ion clusters with increasing water content in the solvent. Under no conditions were solvated electrons observed in zeolites devoid of water in the sodalite cage and bathed in anhydrous solvents. This study shows for the first time the formation of solvated electrons in the zeolites X and Y in solvents other than water.

References and Notes

(1) Kasai, P. H. *J. Chem. Phys.* **1965**, *43*, 3322.
(2) Rabo, J. A.; Angell, C. L.; Kasai, P. H.; Schomaker, V. *Discuss. Faraday Soc.* **1966**, 328.
(3) Kasai, P. H.; Bishop, R. J., Jr. *J. Phys. Chem.* **1973**, *77*, 2308.
(4) Edwards, P. P.; Anderson, P. A.; Thomas, J. M. *Acc. Chem. Res.* **1996**, *29*, 23.
(5) Barrer, R. M.; Cole, J. F. *J. Phys. Chem. Solids* **1968**, *29*, 1755.
(6) Haug, K.; Srdanov, V.; Stucky, G.; Metiu, H. *J. Chem. Phys.* **1992**, *96*, 3495.
(7) Blake, N. P.; Srdanov, V.; Stucky, G. D.; Metiu, H. *J. Phys. Chem.* **1995**, *99*, 2127.
(8) Iu, K. K.; Thomas, J. K. *J. Phys. Chem.* **1991**, *95*, 506.
(9) Iu, K. K.; Thomas, J. K. *Colloids Surf.* **1992**, *63*, 39.
(10) Iu, K.-K.; Liu, X.; Thomas, J. K. *J. Photochem. Photobiol., A* **1994**, *79*, 103.
(11) Liu, X.; Thomas, J. K. *J. Chem. Soc., Faraday Trans.* **1995**, *91*, 759.
(12) Liu, X.; Iu, K.-K.; Thomas, J. K. *Chem. Phys. Lett.* **1994**, *224*, 31.
(13) Takatani, S.; Fukumura, H.; Masuhara, H.; Hashimoto, S. *J. Phys. Chem. B* **1997**, *101*, 3365.
(14) Liu, X.; Zhang, G.; Thomas, J. K. *J. Phys. Chem.* **1995**, *99*, 10024.
(15) Liu, X.; Iu, K.-K.; Thomas, J. K. *J. Phys. Chem.* **1994**, *98*, 13720.
(16) Liu, X.; Zhang, G.; Thomas, J. K. *J. Phys. Chem. B* **1997**, *101*, 2182.
(17) Zhang, G.; Liu, X.; Thomas, J. K. *Radiat. Phys. Chem.* **1998**, *51*, 135.
(18) Thomas, J. K. *Chem. Rev.* **2005**, *105*, 1683.
(19) In this manuscript, the term "trapped electron" refers to electrons trapped by either solvent clusters or ion clusters. The former are referred to as "solvated electrons" and the latter as "ion cluster trapped electrons". Trapped electrons are sometimes referred to as "excess electrons" and can be distinguished from quasi-free electrons from which trapped electrons are derived.
(20) Breck, D. W. *Zeolite Molecular Sieves: Structure, Chemistry, and Use*; Wiley-Interscience: New York, 1974.
(21) Ward, J. W. *ACS Monogr.* **1976**, *171*, 118.
(22) Bertsch, L.; Habgood, H. W. *J. Phys. Chem.* **1963**, *67*, 1621.
(23) Hashimoto, S.; Miyashita, T.; Hagiri, M. *J. Phys. Chem. B* **1999**, *103*, 9149.
(24) Ellison, E. H. *J. Phys. Chem. B* **2004**, *108*, 4607.
(25) Kalyanasundaram, K.; Thomas, J. K. *J. Am. Chem. Soc.* **1977**, *99*, 2039.
(26) Dorfman, L. M. *Adv. Chem. Ser.* **1965**, *50*, 36.
(27) Bell, I. P.; Rodgers, M. A. J.; Burrows, H. D. *J. Chem. Soc., Faraday Trans. 1* **1977**, *73*, 315.
(28) Shkrob, I. A.; Sauer, M. C., Jr. *J. Phys. Chem. A* **2002**, *106*, 9120.
(29) Albery, W. J.; Bartlett, P. N.; Wilde, C. P.; Darwent, J. R. *J. Am. Chem. Soc.* **1985**, *107*, 1854.
(30) Thomas, J. K. *Chem. Rev.* **1993**, *93*, 301.
(31) Murov, S. L.; Carmichael, I.; Hug, G. L. *Handbook of Photochemistry*; Marcel Dekker: New York, 1993.
(32) Birks, J. B. *Photophysics of Aromatic Molecules*; Wiley Monographs: New York, 1970.
(33) Hashimoto, S.; Mutoh, T.; Fukumara, H.; Masuhara, H. *J. Chem. Soc., Faraday Trans.* **1996**, *92*, 3653.
(34) Reichardt, C. *Solvents and Solvent Effects in Organic Chemistry*; Wiley-VCH: Weinheim, Germany, 2003.
(35) Hashimoto, S. *Mol. Supramol. Photochem.* **2000**, *5*, 253.
(36) Barthomeuf, D. *J. Phys. Chem.* **1984**, *88*, 42.
(37) Barthomeuf, D. *Catal. Rev.—Sci. Eng.* **1996**, *38*, 521.